Design and testing of a propeller for a two-seater aircraft powered by fuel cells

G Romeo, E Cestino, M Pacino, F Borello and G Correa

Proceedings of the Institution of Mechanical Engineers, Part G: Journal of Aerospace Engineering 2012 226: 804
originally published online 16 September 2011
DOI: 10.1177/0954410011415476

Design and testing of a propeller for a two-seater aircraft powered by fuel cells

G Romeo, E Cestino*, **M Pacino, F Borello,** and **G Correa**
Department of Aerospace Engineering, Politecnico di Torino, Torino, Italy

The manuscript was received on 17 March 2011 and was accepted after revision for publication on 9 June 2011.

DOI: 10.1177/0954410011415476

Abstract: This article deals with the design, manufacturing, and testing of a propeller for a general aviation aircraft fuelled by hydrogen. The feasibility of the ENFICA-FC project depended on several key-enabling technologies. In order to minimize the power required from both the batteries and the fuel cell, a highly efficient electrical propulsion system was required, in which all the components would need to yield the highest possible efficiency. The choice of the propeller for this specific aircraft was more difficult, above all because the electric motor was limited as to the torque it could handle. In addition, the propeller would also have to provide the necessary airflow for the motor, electronics, and fuel cell cooling to ensure that the temperature did not exceed the limits imposed by the manufacturer. Although a designer may be aided by modern numerical design and analysis programmes to optimize propellers, structural and manufacturing constraints can influence the final choices. Finally, the calculated performance would always have to be validated with experimental tests. An optimal propeller has been designed and manufactured to be installed on the Rapid 200 FC aeroplane. Static tests on the manufactured two-blade propeller were performed by means of a static test facility. Specific tests have also been performed to check the efficiency of the propeller when installation effects (blockage and scrubbing drag effects) are included and to verify the real efficiency of the propulsion and cooling systems, with the propeller installed in the complete converted aircraft. A good agreement between the theoretical and experimental data was obtained.

Keywords: fuel cell aircraft, CFD analysis, propeller design

1 INTRODUCTION

Because of their high energy density, proton exchange membrane (PEM) fuel cell systems are becoming increasingly attractive as the primary power plant for low-power, long-endurance aircraft applications. Fuel cells offer several advantages over conventional sources for the generation of electricity. As an electrochemical device, fuel cells have much higher potential efficiency than heat engines. Fuel cells have no moving parts and are silent although some external devices, such as blowers and pumps are usually required to deliver the reactants and manage the temperature. The basic design allows fuel cells to be highly scalable and a number of potential fuel sources are available. Direct hydrogen PEM fuel cells could offer the advantage of high power density and short start-up time. Using pure hydrogen as fuel, water is the only emission product allowing to obtain a 'zero emission' system. While other types of fuel cells and/or with different types of fuels are used, also produce other hydrides, although in much smaller quantity of a combustion engine, and therefore are referred to 'near zero emission'.

The primary benefits of fuel cells for aircraft applications are high efficiency, quiet operation, the lack of the necessity of a generator to produce electricity, and ease of scalability [**1**].

**Corresponding author: Department of Aerospace Engineering, Politecnico di Torino, Corso Duca degli Abruzzi 24, 10129 Torino, Italy.*
email: enrico.cestino@polito.it

A small fuel cell-powered aeroplane was designed and constructed at the Georgia Institute of Technology in 2005 [**2**] to develop a system design method for fuel cell-powered unmanned aerial vehicles. A 448 -W net output PEM fuel cell power plant was constructed and flight-tested.

In February and March 2008, the Boeing Company [**3**] successfully performed flight tests on the first manned fuel-cell motor-glider in aviation history. The fuel-cell demonstrator aeroplane was a modified two-seater motor-glider equipped with a hybrid power source powering an electric motor that drove a variable-pitch propeller.

In July 2009, a German motor-glider became the first piloted aircraft to take off under only fuel-cell power [**4**]. The Antares DLR-H2, developed by the German Aerospace Center (DLR), took off from Hamburg Airport. This glider is a hydrogen-powered variant of the Antares 20 E electric motor-glider and has a 66-ft wingspan. The plane achieved 105 mile/h.

The EC-funded project ENFICA-FC (ENvironmentally Friendly Inter City Aircraft powered by Fuel Cells) [**5**–**8**] has the aim of obtaining a better understanding of the problems related to fuel cells applied in aeronautics. The main objective of the ENFICA-FC project was to develop and validate the use of a fuel cell-based power system for the propulsion of several more/all electric aircrafts. The fuel cell system was installed on the light RAPID 200 sports aircraft, the first aeroplane (FAI Sporting Code Category C) to fly and be performance-tested. Six test flights were successfully carried out by the Politecnico di Torino. The all-electrical power system was successfully tested during experimental flights in May–June 2010. Considering an asphalt runway and aeroplane in its maximum mass configuration (about 550 kg), a rotation speed of about 23 m/s was obtained for a ground roll distance of 184 m. Maximum speed at level flight was attained at about 43 m/s, only by means of a fuel cell power setting. A new speed world record of 37.5 m/s and an endurance of 39 min were established during several flights for the FAI Sporting Code Category C (aeroplane) [**6**, **7**]. The positive handling qualities and satisfactory engine performances of these six flight tests led the team to consider these successful flights as a good starting point for further long-endurance high-speed flights.

The use of a propeller to generate thrust for subsonic flight dates back to the beginning of powered flight. The application of propellers to generate thrust, under most flight conditions, is already fully understood, due to the long history of its use and development. However, for particular applications, such as for innovative 'environment-friendly aircraft', very little knowledge is available. Most of the existing propellers were designed for the conventional piston engines that are usually used for the ultra-light category of aeroplanes.

This article deals with the design, manufacturing, and testing of a propeller for the general aviation aircraft, fuelled by hydrogen that was designed and tested during the ENFICA-FC Project. The torque provided by an electric motor is directly connected to the current that is supplied to the motor itself, which is physically limited to the amount of current it can handle. This means that the propeller needs to work with a relatively high r/min to absorb the

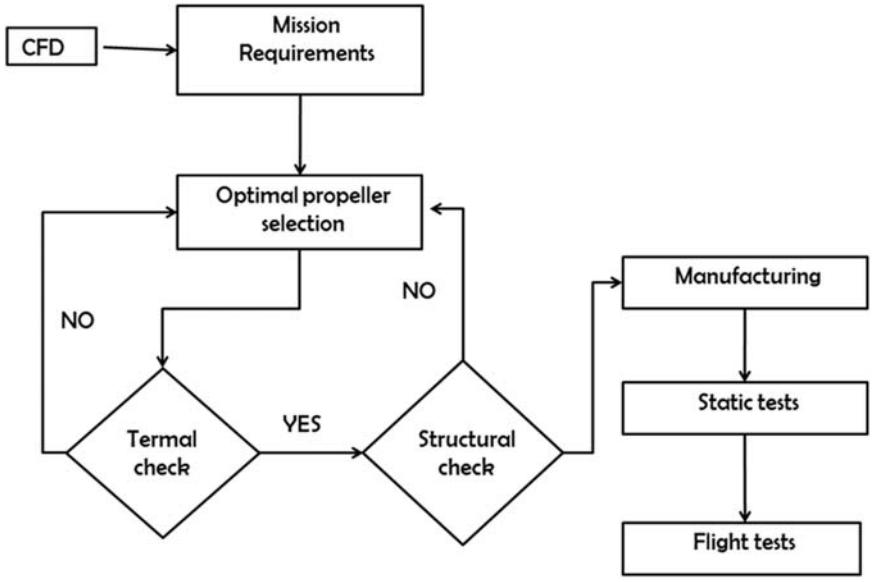

Fig. 1 Propeller design process

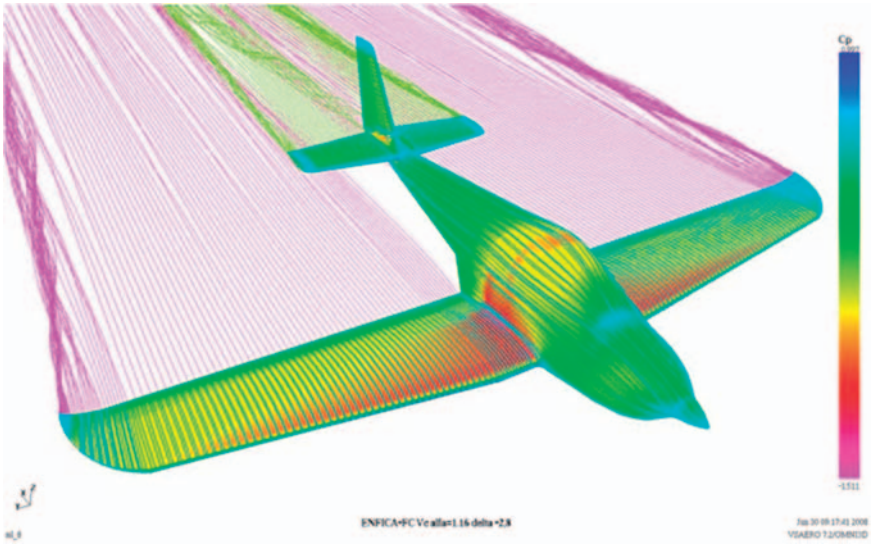

Fig. 2 CFD analysis

available power. One of the most critical, if not the most critical, aspects of the all-electric power system adopted as the demonstrator is undoubtedly cooling; the reduced volumes and low weights that are needed for aeronautical applications are not beneficial from a heat-management point of view and hence cooling design and prediction becomes a challenging key activity for the whole flight test campaign.

An optimal propeller was designed and manufactured in order to transfer the power produced by the motor to the air stream as efficiently as possible and to provide an adequate flow to the engine cowl air intake for cooling purposes (Fig. 1). A low induced velocity at the propeller disc increases the ideal efficiency but, on the contrary, a low value of the slipstream velocity could be critical for the cooling system.

Static tests were performed on the manufactured two-blade propeller in a static test facility. Specific tests were also performed with the propeller installed in the complete converted aircraft to check the efficiency of the propeller when installation effects were included and to verify the real efficiency of the propulsion and cooling systems.

2 REQUIREMENTS OF THE MISSION

The propulsion system configuration of the converted aircraft includes: (a) battery, (b) fuel cell system, (c) H2 system, (d) DC/DC converter, and (e) DC/AC converter. About 20 kW of power should be provided by the fuel cell stack and an additional 20 kW should be provided by the batteries. The battery pack should work for about 15 min to boost the aircraft during take-off and the initial climb from 0 to 1000 m. The overall system should weigh no more than 221 kg. A complete, but limited, mission profile was selected by the consortium as in references [**6**, **7**], since the goal was to show the feasibility of a new concept propulsion system. The mission can be summarized as follows:

(a) take-off;
(b) climbing up to 1000 m with a climbing rate of 2.5 m/s;
(c) cruising over the airport at approximately 40 m/s for 40 min;
(d) descending and landing.

The requested mission performances were based on a parametric study; system architecture design and mission properties were chosen because they could guarantee that the mission could be flown while keeping the total mass at around 550 kg, i.e. the maximum total mass at which the original RAPID200 was tested. This result was confirmed at the end of the conversion activity [**7**]. A better understanding of the aerodynamic behaviour of the aircraft was needed to define the power requested for the mission phases; a computational fluid dynamics (CFD) analysis was performed (Fig. 2) for this purpose, by means of the VSAERO commercial code [**9**]; the analysis concerned not only the overall aircraft, but also the critical components that had to be designed; as an example, the CFD results were vital

for the design of the engine cowl [**8**] which had to guarantee a proper cooling of the different systems installed in the engine bay, but also act as a passive safety system for the prevention of hydrogen accumulation. Moreover, the CFD results were important to design the complete hydrogen venting system and to predict the best locations for the static pressure ports.

The requested power (including efficiencies of propeller, motor, and inverter/converter) at a cruising speed of about 40 m/s was about 18 kW and the requested power for climbing at 2.5 m/s resulted to be about 37 kW.

There are various types or classes of propellers, the simplest of which are fixed-pitch or ground-adjustable propellers. Obviously, the more complex propellers provide better performance over a wider range of operating conditions, as their blade angle can be adapted to the specific operating conditions. Fixed-pitch propellers are simple propellers whose blade angle cannot be changed during normal operations. They are usually found on light, single-engine aeroplanes and are usually made of wood, aluminium, or composite materials. Fixed-pitch propellers are designed because of their better efficiency at one rotational and forward speed. They are only designed to fit one set of aeroplane and engine speed conditions. Any change in these conditions will reduce the efficiency of both the propeller and the engine. Since the objective of the ENFICA-FC project was to conduct an experimental flight, the propeller had to work in a few different conditions. A fixed propeller solution was chosen and the optimized blade was designed for two different conditions: cruising (case A) and climbing (case B), as indicated in Table 1.

Table 1 Design requirements

	Case A (cruising)	Case B (climbing)
Altitude (ISA model) (m)	1000	500
Flight speed (TAS) (m/s)	40	33
Angular speed (r/min)	2000	2000
Required thrust (N)	340	780
Blade radius (m)	0.8	0.8
Number of blades	2–3	2–3

However, the propeller did not only have to match the propulsive requirements of the aircraft. Its characteristics also had to fit the engine's torque–speed curve. The engine needed to be able to deliver the required torque to turn the propeller.

The propeller selected must be appropriate for engine performance characteristics throughout the r/min range. For instance, the propeller must absorb all the engine torque for a specific r/min and throttle setting. If does not, then the engine will accelerate and an increase in airspeed may cause the propeller to overspeed, causing loss of performance or even damage to the engine. The opposite will happen if the propeller absorbs more torque than the engine is supplying. The ideal match is when propeller curve intercepts engine curve at nominal maximum r/min. This means that while the propeller is rotating at speed below its maximum, there is always sufficient surplus engine torque to accelerate the propeller to maximum speed when full throttle is opened up [**10**].

The reader can refer to reference [**11**] for more details on the ENFICA air-cooled brushless engine and consider a maximum engine rotational speed of about 3000 r/min with a torque of 150 Nm. Another key aspect of the propeller design was the cooling system requirements and the evaluation of the motor/electronics and fuel cell temperature. The motor was cooled by air forced through the frontal intakes; this involved some modifications of the original leading-edge profile of the engine cowl. The requested air had to be no less than 2 m^3/min in the preparatory phase up to 20 m^3/min during climbing and level flight operations. The constructor's specifications indicated a maximum environment temperature of 40 °C and an operating temperature of 120°C.

The aircraft power management unit was basically composed of a DC/DC converter (chopper), a DC/AC inverter, and a controlling logic unit piloting the power-related devices.

The inverter had the purpose of controlling the electric motor in terms of output power to the propeller. The power electronics specifications indicated values of about 90 °C as a typical maximum operating temperature [**12**].

As far as fuel cell is concerned, as the ionic conduction of the polymeric membrane is a function of its degree of humidification, the stack temperature had to be carefully controlled to avoid water evaporation phenomena which could cause an increase in the ohmic drop and a decrease in the stack performances. The output voltage (and hence the power) of the fuel cell system was affected to a great extent by the change in the stack temperature. For all these reasons, the induced velocity of the propeller had to ensure a sufficient flowrate to maintain temperatures below the limits established by manufacturers during all flight conditions and in particular in the worst condition (take-off), where the speed of the aircraft is very low.

3 DESIGN OF THE OPTIMAL PROPELLER

The main objective of the design of a propeller is to transfer the power produced by the motor to the air

stream as efficiently as possible. The efficiency of the propulsion system in general and of the propeller in particular was the key aspect for the flight tests of the ENFICA FC project as they had a direct and important impact on the power required from the fuel cell and the battery and therefore also on the mass of these components. In order to increase the efficiency of the propeller, the blade diameter should be maximized as shown in equation (1); in fact, when the diameter of the propeller is increased, the delivered power is spread over a larger disc area, and this results in a lower loading of the propeller, which in turn leads to a lower slipstream velocity and thus a higher efficiency. On the contrary, a low value of the slipstream velocity could be critical for the cooling system. Additionally, the diameter is limited by both ground clearance and Mach number constraints. The diameter must, first of all, be kept small enough so that it will not hit the ground during landing to avoid engine and propeller damage. Furthermore, the diameter must be limited to avoid high blade Mach numbers at the tip, as this leads to excessive noise as well as compressibility effects on blade drag, 0.8 is a sensible working maximum Mach number at ISA S/L conditions but a lower value may be beneficial in terms of noise reduction.

The ideal efficiency of a propeller can be deduced using the axial momentum theory, where blade drag effects are neglected [**13**]. Only axial momentum and a uniform increase in velocity over the entire disc area are considered. The ideal efficiency is fixed for a given thrust, flight velocity, and propeller radius, and can be written as

$$\eta_i = \frac{T \cdot V_\infty}{P} = \frac{1}{1 + v_i/V_\infty} \text{ with}$$
$$v_i = \frac{1}{2}\left(\sqrt{V_\infty^2 + \frac{2T}{\rho S}} - V_\infty\right) \quad (1)$$

During the cruising condition, the ideal efficiency is 95 per cent and during the climbing phase it is 88 per cent. It is very important to notice that these two values are the highest that can be obtained and, in practice, considering all the losses, it is impossible to reach these levels.

The optimum propeller efficiency is, instead, the efficiency (excluding energy losses deriving from profile drag or finite wing effects) that has an optimum load distribution as, suggested by Goldstein for a specified number of blades [**14–17**]. The advantage of using this efficiency is that it presents a maximum value that cannot be exceeded for a given propeller diameter and blade number, but which can be obtained through a proper design. A numerical procedure for the determination of an optimal twist angle and chord distribution, as a function of the distance r from the hub, for an n-blade propeller of radius R, is presented in reference [**16**] and used here to derive the geometry of the ENFICA-FC propeller. The optimum propeller will minimize the energy loss to provide the required thrust, considering the operating point in terms of forward speed, propeller angular velocity, and altitude.

The maximum efficiency of the propeller is obtained if all the airfoils along the blade span are at their maximum efficiency angle of attack. The angle of attack for maximum efficiency for each section is determined as a function of the local Reynolds and Mach numbers. The resulting chord and twist angle distributions along the blade depends on four independent parameters τ, γ, Re, and Ma.

The design of the optimized blade requires the *a priori* knowledge of the number of propeller blades. The analysis was carried out for two and three blades. The evaluation of the aerodynamic performance of the propeller and its optimization required detailed knowledge of the airfoil used for the blades which had to provide the drag and lift coefficient values as function of the angle of attack and the Reynolds number [**18**]. A ClarkY profile was selected for the first iteration of the propeller design. An aerodynamic database was created as a function of the angle of attack [$-10°/+25°$] and the Reynolds number [from 10^3 up to 5×10^6] by means of the XFOIL code. The propeller (two blades) optimized in cruising conditions had a radius of 0.8 m, which was chosen equal to the original one in order to respect geometrical bounds, and had a mass of about 4 kg. Considering the cruising parameters indicated in Table 1, for an optimized propeller, the efficiency could reach 90 per cent. The optimal collective pitch angle was equal to 22.8°. Using the same flight conditions, but changing the number of blades ($n = 3$), the efficiency of the propeller did not change to any great extent.

The climbing parameters indicated in Table 1 were adopted to design the blade for climbing conditions. It should be noted that, in this case, the thrust generated from the propeller would equilibrate not only the aircraft drag but also a part of the weight. Since a faster climb was considered, the flight velocity and the thrust required at the propeller changed with the altitude and for this reason, the design of the propeller was carried out at a 'medium' altitude. Considering a two-blade propeller, the efficiency of the propeller reached 80.6 per cent and a collective pitch angle 20.6°. Passing to a three-blade propeller, the maximum efficiency did not differ very much and rose to a value of 81.5 per cent with a collective pitch angle of 20.9°. The result of this first analysis was the chord and twist angle distributions along the radius,

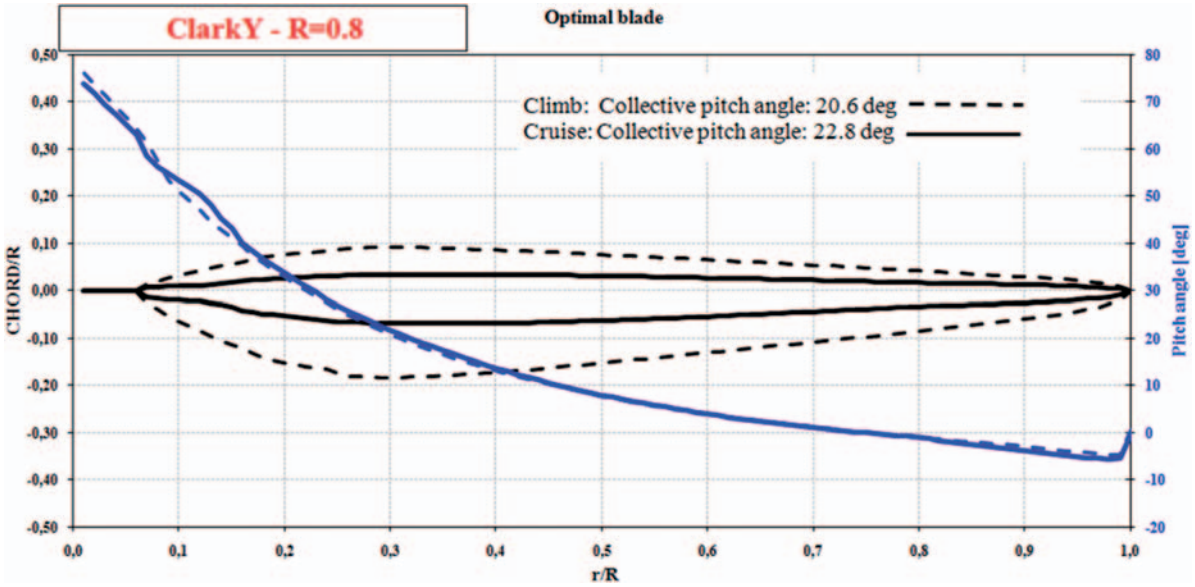

Fig. 3 Optimal two-blade propeller geometry (cruising and climbing)

as shown in Fig. 3, for the case of a two-blade propeller optimized for cruising and climbing conditions.

Using a second algorithm [**16**], it was possible to evaluate the behaviour of the propellers outside the design condition. Fixed-blade propellers were considered and the collective pitch angle was fixed and equal to the optimal one. This means that when the flight condition changed, the angular velocity of the propeller (and therefore the angular velocity of the engine) also had to change. However, different collective pitch angles were also taken into account. Non-dimensional parameters are often used to describe the performance of a given propeller. In this way, a single figure can be used to describe the performance of a propeller under different operating conditions (flight speed, altitude, and r/min). The following parameters were used

$$\gamma = \frac{V_\infty}{\Omega R}\,\tau = \frac{T}{\rho\Omega^2 R^4}\,\chi = \frac{P}{\rho\Omega^3 R^5}\,\eta = \frac{TV_\infty}{P} = \frac{\tau\gamma}{\chi} \qquad (2)$$

The results, in terms of thrust coefficient and efficiency of the optimal two-blade cruising propeller are reported in Fig. 4.

During the climbing phase, the propeller optimized for cruising conditions had to generate a thrust of about 784 N and the aircraft velocity had to be 33 m/s at an altitude of 500 m. Since all the other parameters were fixed, the angular velocity had to change to $\Omega = 2490$ r/min. Similarly, the propeller optimized for climbing, during the cruising phase, had to generate 340 N of thrust with an aircraft velocity of 40 m/s at an altitude of 1000 m. The propeller angular velocity that guaranteed these conditions was equal to $\Omega = 1880$ r/min. A performance summary of the two-blade propellers is given in Table 2. The analysis showed that it was hypothetically possible to obtain a 90 per cent efficiency propeller for cruising conditions and about 80 per cent for climbing conditions. These results are quite good compared with the maximum theoretical efficiency that can be reached in such conditions. Due to the fact that less energy is consumed during the mission, the two-blade optimized version for cruising was selected for manufacturing.

4 PROPELLER MANUFACTURING AND PERFORMANCE COMPARISON

A propeller builder, GT propellers, was contacted and asked to build a propeller for the Rapid 200-FC. According to the manufacturer, it was not possible to build the designed optimal propeller using the present technology because of the too thin aspect ratio related to the forces that had to be tolerated. Because of this, the builder presented a series of five modified propeller geometries which, in his opinion, could satisfy the requirements.

The first two propeller geometries were called GT166 (T1) and GT 166-slim version (T2) (Fig. 5); they had the same chords and twist, but different airfoil thicknesses. These geometries were analysed with the same algorithm used for the optimal propeller in order to make a result comparison possible. The new propellers both had 5 per cent less efficiency in cruising condition than the optimal one, while during climbing, the efficiency seemed to be almost the

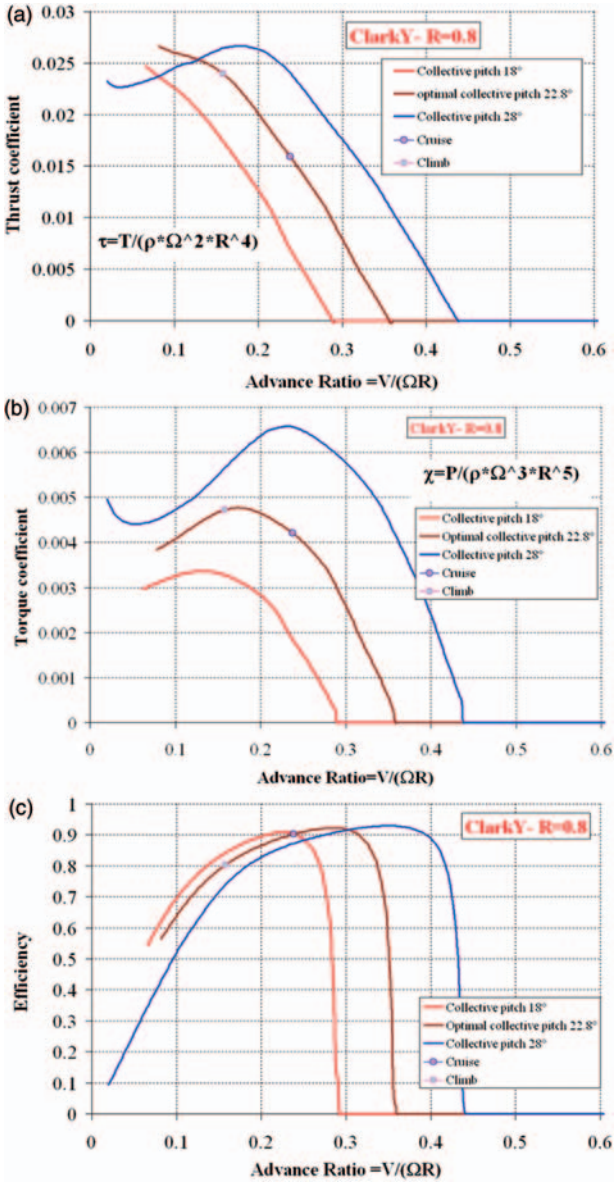

Fig. 4 Thrust and power coefficient and efficiency of the optimal cruising two-blade propeller

same but with a lower r/min. In the climbing condition (Fig. 6), the two new propellers required an r/min value of almost 20 per cent less than the optimal propeller to generate the same thrust.

Comparing the power required to give the climb thrust with respect to the optimal propeller, T1 needed the same power as the optimal propeller, while T2 needs more power. However, as observed before, both propellers generated this thrust and power at lower r/min than the optimal one.

Comparing the thrust at cruising speed (Fig. 7), T1 would run at 10 per cent less r/min that the optimal propeller for the cruise thrust, while T2 would run at 5 per cent less. T1 and T2 required about 5 per cent more power than the optimal propeller.

The two GT propellers seemed to have similar performances but T2 required a little more power to climb, otherwise it would have run at higher r/min values than T1, which is better for motor requirements. The critical aspect for the hydrogen flight concerns the cruising condition, where the propulsion power had to reached by fuel cells alone; T2 was therefore chosen as it was considered more convenient to keep the r/min higher than to earn a reduction of a few watts in the climbing phase during which the batteries also supply power.

Starting from the T2 geometry, three more propellers were analysed in order to investigate the cruising performance variations with a change of the propeller geometries. Two propellers were designed by varying the twist (T3 and T4) and the last one (T5) by varying the chord distribution. All of them were designed taking into account the 'manufacturability' of the propeller.

The T3 propeller obtained the same efficiency as the T2 one in climbing conditions, but reached a lower efficiency than the T2 one in cruising conditions.

The T3 torque was between the T2 and optimal ones for climbing, while T4 had a similar torque to T2. As the objective was to minimize power in the cruising phase, the two new propellers, T3 and T4, resulted to be less efficient than T2.

A last attempt was made to try to improve the performances by reducing the T2 chords near the root. This modified version was called T5. This last version also resulted to be less efficient during the cruising phase and the T2 propeller was therefore chosen for the required flight conditions as it was considered the best compromise to obtain good cruise efficiency.

Considering the results of all the analyses as shown in Table 3 and taking into account that propellers with very small root chords cannot be manufactured with the current technology, the best propeller for the considered application, from all the propellers proposed by the builder, appeared to be the T2 GT 166-Slim version. The propeller was built by the manufacturer, GT Propeller, in a composite and wood material. It is not possible to report all the manufacturing details in order to respect the manufacturer's confidential know-how. The final result was to obtain a very light propeller (mass = 2.0 kg) with a reduction in mass compared to traditional propellers (4 kg).

5 STATIC TESTS ON THE PROPELLER

In order to verify the analytical results, the propeller was subjected to static tests, before being installed on

Table 2 Optimization results

		Propeller 1	Propeller 2
Optimized for		Cruising	Climbing
Number of blades		2	2
Radius (m)		0.8	0.8
Collective pitch angle (°)		22.8	20.6
Climbing phase	Advance ratio	0.158	0.197
	Efficiency (%)	80.2	80.6
	Thrust coefficient	0.0240	0.0373
	Torque coefficient	0.004 72	0.009 01
	Thrust (N)	782	784
	Torque (Nm)	123	153
	Power at the shaft (kW)	32.1	32
	Angular velocity (r/min)	2490	2005
Cruising phase	Advance ratio	0.239	0.254
	Efficiency	90	88.4
	Thrust coefficient	0.0170	0.0198
	Torque coefficient	0.004 50	0.005 68
	Thrust (N)	340	349
	Torque (Nm)	72	80.2
	Power at the shaft (kW)	15.1	15.8
	Angular velocity (r/min)	2040	1880
Total energy consumed	Entire mission energy consumed (kWh)	13.81	14.27

Fig. 5 GT 166 propeller geometry

board the aircraft. The experiment was performed in the laboratory and test facility of NAUTILUS SPA at the Reggio Emilia airport where the aeroplane was tested. All the systems were already calibrated and the tested machine was composed of a metallic structure which supported the propeller shaft at the top and the electric motor at the bottom. The r/min of the motor was reduced to the propeller shaft by belt transmission. The maximum torque that was measured was 170 ± 0.2 Nm, the maximum thrust 2000 ± 5 N, and the maximum angular velocity 9000 r/min. When thrust was generated by the rotation of the propeller, the entire system moved forward slightly; a load cell was used for the thrust measurements while the others parameters were deduced from the motor voltage and current.

Figure 8 shows the Nautilus testing machine with the tested propeller.

Three tests, with a total of five measurements, were made for the GT propeller (T2). In two tests, the measurements were performed during both phases: increasing and the decreasing the motor speed; in one test, the data were only taken during the increasing phase. The data from the five test sets are plotted in Figs 9 and 10, together with the numerical predictions.

The numerical results were obtained with the VSAERO-Rotor computer code [**19**], a CFD panel method, coupled to a blade element method which was used to calculate the performance of the rotor. Numerical results were validated only in the static case.

If the five measurements and numerical results are compared, a close match can be observed between designed propeller and the one realized.

The solid line in Fig. 9 is a curve that starts from zero thrust with zero rotation and runs to approximately 120 kg at 1700 r/min. The experimental data match and show a good agreement with the numerical results until 1700 r/min; after this value, the transmission belt on the test machine began to slip.

Figure 10 shows the relationship between the torque required to operate the motor and the r/min for which that particular torque operates. As in the previous figure, the solid line illustrates the values of the torque predicted by the CFD-numerical analysis, while the particular points of data show the values obtained experimentally. In this case, the correlation between the theoretical and experimental torque trends is not as close as the previous case, but still accurate enough for design purposes. This is due to the fact that more energy was required to turn the propeller than predicted, because the theory did not take into account all the drag forces which must be overcome to spin the propeller.

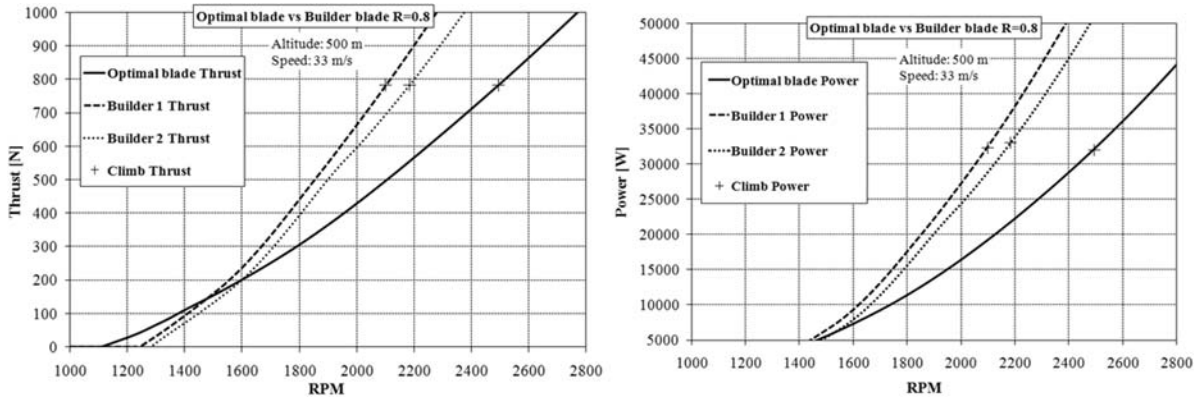

Fig. 6 Thrust and power comparison – climbing

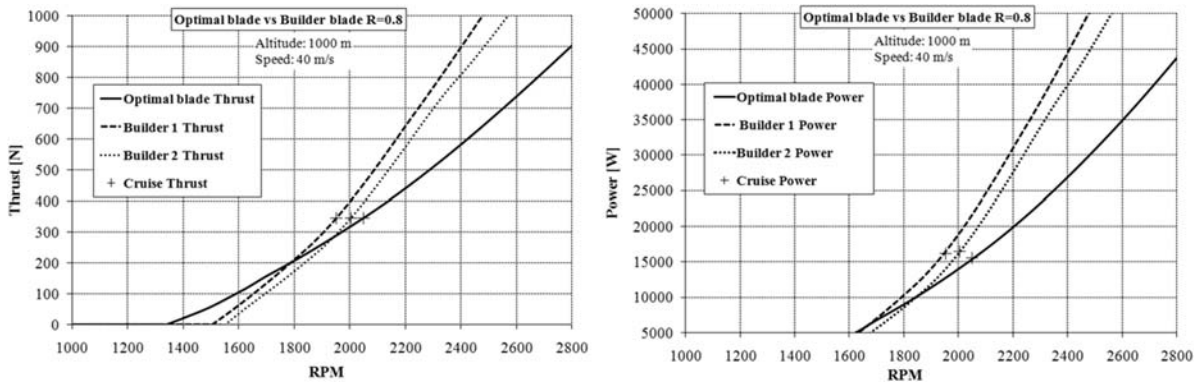

Fig. 7 Thrust and power comparison – cruising

Table 3 Builder's propellers comparisons

Type	Chord	Airfoil thickness	Twist angle	Power (cruise)	Power (climb)	r/min (cruise)	r/min (climb)
T1	$=$T2	$>$T2	$=$T2	$\approx$T2 $>$ OPT	$\approx$OPT $<$ T2	$<$OPT $<$ T2	$<$OPT $<$ T2
T2 (selected)	—	—	—	$>$OPT	$>$OPT	$<$OPT	$<$OPT
T3	$=$T2	$=$T2	$\neq$T2	$>$T2 $>$ OPT	$\approx$T2 $>$ OPT	$>$T2 $>$ OPT	T2 $<$ T3 $<$ OPT
T4	$=$T2	$=$T2	$\neq$T2 $\neq$ T3	$>$T2 $>$ OPT	$\approx$T2 $>$ OPT	$>$T2 $>$ OPT	$\approx$T2 $<$ OPT
T5	$\neq$T2	$=$T2	$=$T2	$>$T2 $>$ OPT	$>$T2 $>$ OPT	$<$T2 $<$ OPT	$<$T2 $<$ OPT

6 STATIC TESTS ON THE INSTALLED PROPELLER

The real propeller performance and efficiency of the cooling systems (FC, motor, and power electronics) were checked with the complete system installed onboard the aeroplane (Fig. 11).

The previous tests were concerned with the performance of the propeller in free air, without considering for any disturbing influence on the propeller inflow and slipstream. In reality, a propeller is always attached to an engine which is mounted onto either the aircraft fuselage or onto a nacelle attached to the wing, fuselage, or tail unit. The presence of the body to which the propeller is attached (i.e. a nacelle or fuselage) modifies the flow field through the propeller. In addition, the flow generated by the propeller increases the drag of the body. In order to account for

the delay in the airflow through the propeller discs, which is caused by the presence of the fuselage behind the propeller, an effective advance ratio is frequently introduced, as in reference [**13**]

$$\gamma_{\text{eff}} = (1-h)\gamma = \left(1 - 0.329 \cdot \frac{S_{\text{body}}}{D^2}\right)\gamma \tag{3}$$

where h accounts for the delay in the flow through the propeller disc caused by the body behind it and which is given by an empirical relation. The part of the fuselage or wing that is located directly in the slipstream will also undergo a change in drag, which is called 'scrubbing drag'. This effect can be considered an increase in aeroplane drag or a decrease in the installed thrust of the propeller. An effective thrust can be computed through the definition of a scrubbing factor F, which is defined as [**13**]

$$F = \frac{T_{\text{eff}}}{T_{\text{isolated}}} = 1 - 1.558\frac{\rho/\rho_0 \cdot f_{\text{slip}}}{D^2} \tag{4}$$

where ρ/ρ_0 is the atmospheric density ratio and f_{slip} the parasite drag area of those components that are immersed in the propeller slipstream. This parasitic area may be estimated from $f_{\text{slip}} \approx 0.004 \cdot S_{\text{wet,slip}}$, where 0.004 0 is an average skin friction coefficient.

Static tests were performed with the aeroplane being held by a load cell (Fig. 12), and the brakes left free while the throttle increased. The tests were conducted with the two-blade GT propeller reaching 20 kW using the fuel cells and then adding battery power to reach 39 kW. The maximum thrust obtained in this configuration was 940 N (95.8 kg). The friction forces of the wheels should also be added to this value; this contribution was estimated by pulling the plane from the load cell with an increasing force and taking the value corresponding to the moment before the tyres began to move. The obtained value resulted to be about 300 N; therefore, the thrust of the GT propeller at 39 kW in static conditions would result in about 1240 N (126 kg).

Figure 13 shows the trend of the experimental thrust as a function of the angular speed; it is possible to notice that, at low speeds, the values are very close

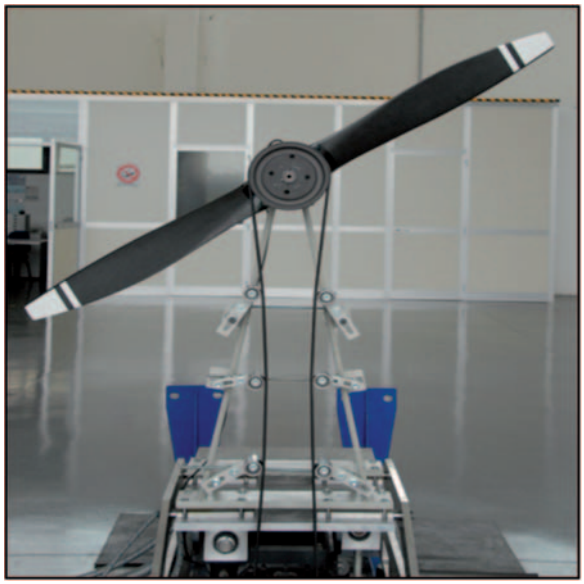

Fig. 8 Propeller test facilities at Nautilus S.P.A

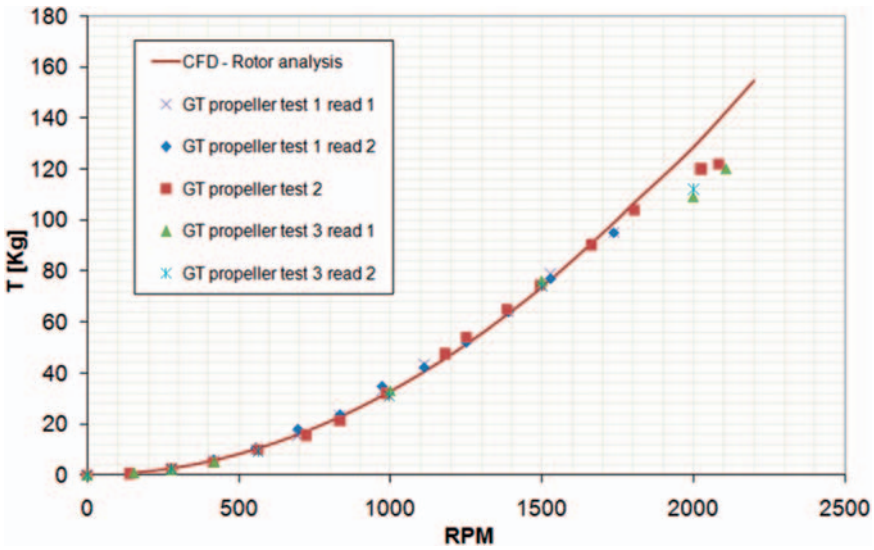

Fig. 9 Thrust production versus r/min

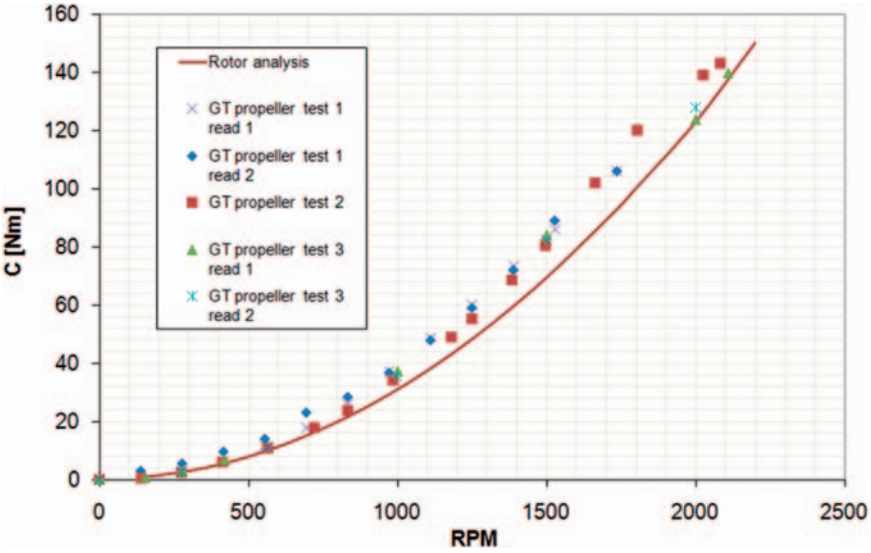

Fig. 10 Torque required versus r/min

Fig. 11 Final propeller/engine cowl installation ready for static tests on the aeroplane

Fig. 12 Static tests on the aeroplane

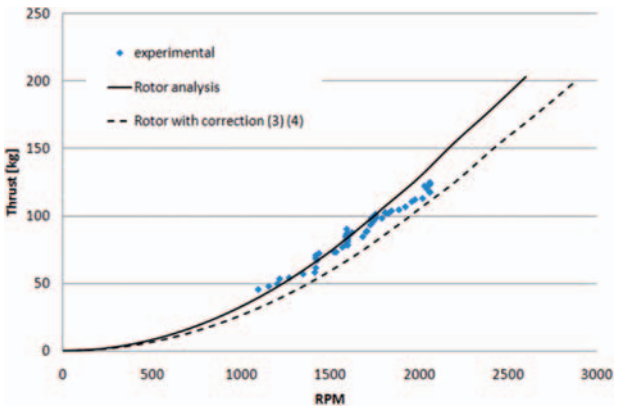

Fig. 13 Final propeller/engine cowl installation thrust of the aeroplane

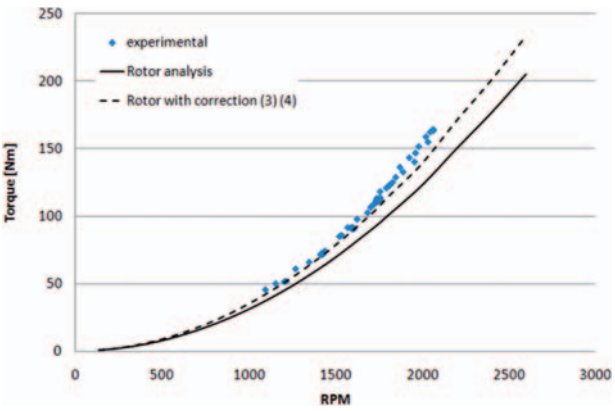

Fig. 14 Final propeller/engine cowl installation torque of the aeroplane

to the numerical values obtained without the effect of the propeller installation, while at high speeds, the effect of the installation starts to become more evident and the dotted curve seems to better approximate the experimental data. The effect of the installation is also reflected in an increase in torque and power, as shown in Fig. 14.

The test on the complete aircraft made it possible to test the quality of the cooling system; the maximum temperatures recorded were about 20 °C for the motor, 40 °C for the inverter, and 60° for the fuel cell stack, confirming the theoretical results presented in references [**8**] and the good behaviour of the cooling system (Fig. 15).

A new world speed record of 135 km/h and endurance of 39 min was established by the Rapid 200 FC, with this propeller mounted, during several flights for Category C (aeroplane) of the FAI Sporting Code (Fig. 16). The previous record established by the Boeing Research & Technology Centre (Madrid) in the first manned fuel cell-powered flight in the world; the single-engine propeller-driven motor-glider Super-Dimona (Class D, FAI Sporting Code), modified by replacing its combustion engine with FCs and an electric motor, flew for about 20 min at maximum speed of 120 km/h; DLR also flew in July 2009 with the motor-glider Antares20-E (Class D, FAI Sporting Code) powered solely by FCs also during take-off and climbing.

Higher speeds than 135 km/h were measured several times, with peaks up to 160 km/h (during the official flight reported in Fig. 16) and 180 km/h during other free flights.

7 CONCLUSIONS

The extensive experimental campaign carried out during the ENFICA-FC project, as well as the theoretical estimations, have proven that FC technologies represent a promising future innovation in aeronautics as a key-enabling technology for all-electric, zero emission, low-noise aircraft.

An optimal two-blade propeller has been designed and manufactured to be installed on the Rapid 200 FC aeroplane, transferring the power produced by the motor to the air stream as efficiently as possible and providing an adequate flow to the engine cowl air intake for cooling purposes. Static tests were performed on the manufactured two-blade propeller in a static test facility. The experimental data matched very well and showed good agreement with the numerical results that were obtained for a static case by means of a CFD panel method coupled to a blade element method. The presence of the body to which the propeller was attached modified the flow field and introduced installation effects that were measured during static tests on the complete aircraft. The test on complete aircraft confirmed the ability of the cooling system to maintain temperatures below the limits established by the manufacturers. A new world speed record of 135 km/h and endurance of 39 min was established by the Rapid 200 FC, with this propeller mounted, during several Category C

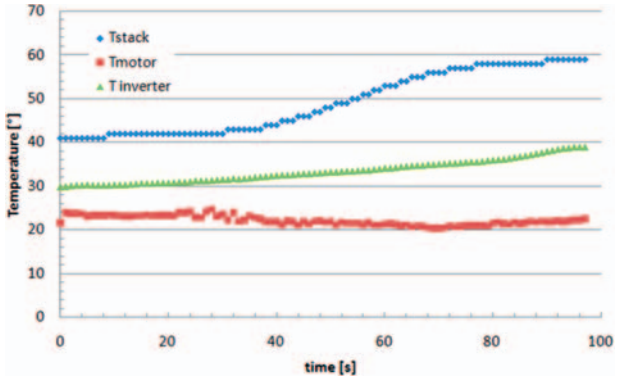

Fig. 15 Final propeller/engine cowl installation temperature of stack, motor, and inverter

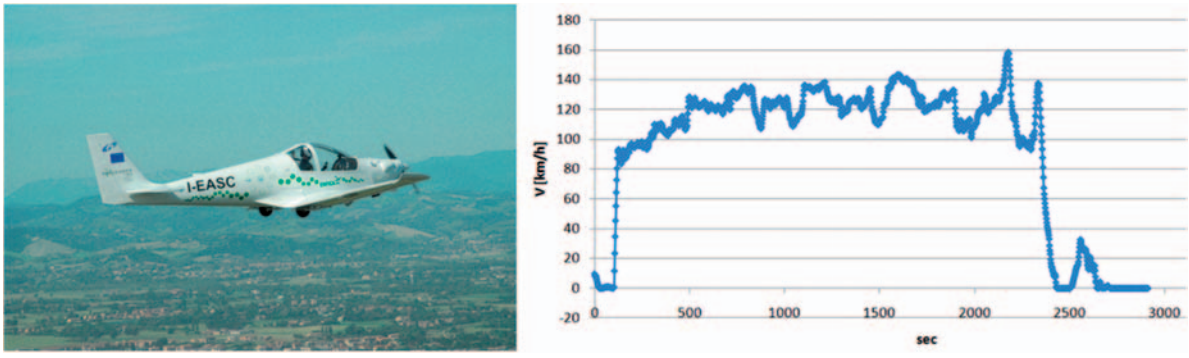

Fig. 16 Rapid 200 FC during record flight

(aeroplane) flights of the FAI Sporting Code. The results obtained during the flights can be considered as a further step in the European and World Aeronautics Science field towards introducing completely clean energy (zero emission).

FUNDING

The activity has been developed as part of the ENFICA-FC project. The writers would like to acknowledge the important contribution made by the European Commission through the ENFICA-FC, EC 6th FP funding programs – contract no. AST5-CT-2006-030779.

REFERENCES

1 **Glover, B.** Fuel cells opportunity. In Proceedings of *AIAA/AAAF aircraft noise and emissions reduction symposium*, Monterey, California, 24 May, 2005.
2 **Bradley, T., Moffitt, B., Thomas, R., Mavris, D.,** and **Parekh D.** Test results for a fuel cell-powered demonstration aircraft. SAE technical paper 3092, 2006.
3 **Lapeña-Rey, N., Mosquera, J., Bataller, E.,** and **Ortí, F.** First fuel-cell manned aircraft. *J. Aircr.*, 2010, **47**(6), 1825–1835.
4 **DLR.** 2009, available from http://www.dlr.de/en/desktopdefault.aspx/tabid-1/86_read-18278/
5 **Romeo, G., Borello, F., Cestino, E., Moraglio, I., and Novarese C.** ENFICA-FC environmental friendly inter-city aircraft and 2-seat aircraft powered by fuel cells electric propulsion (DEU). In Proceedings of the *AIRTEC 2nd international conference*, Frankfurt, Germany, 24–25 October 2007, vol. II, pp. 507–517 (AIRTEC, Frankfurt).
6 **Romeo, G.** and **Borello, F.** Design and realization of a 2-seater aircraft powered by fuel cell electric propulsion. *Aeronaut. J.*, 2010, **114**(1155), 281–297.
7 **Romeo, G., Borello, F.,** and **Correa, G.** Set-up and test flights of an all-electric 2-seater aeroplane powered by fuel cells. *J. Aircr.*, 2011, in press. DOI: 10.2514/1.C031271.
8 **Romeo, G., Cestino, E., Borello, F.,** and **Correa, G.** Engineering method for air-cooling design of 2-seat propeller driven aircraft powered by fuel cells. *J. Aerosp. Eng.*, 2011, **24**, 79–88.
9 **Natham, J. K.** A code for calculating the nonlinear aerodynamic characteristic of arbitrary configuration. In *VSAERO user's manual* version 6.2, 2005 (Analytical Methods, Inc., Washington, USA).
10 British Microlight Aircraft Association: Technical information N.011 Issue:2, January 1999. Available from http://www.bmaa.org/pwpcontrol.php?pwpID=3922.
11 **Romeo, G.** and **Novarese C.** Preliminary choice, based on all available data, of a cots electric drive (motor and inverter), Politecnico di Torino, Italy, 2007.
12 **Power One**. Cooling DC-DC converters power-one application note, 2007, available from http://www.power-one.com.
13 **Torenbeek, E.** *Synthesis of subsonic airplane design Delft*, 1976 (Delft University Press, New York).
14 **Munk, M. M.** *Notes on propeller design I: the energy losses of the propeller*, 1922 (District of Columbia, NASA, Washington).
15 **Reissner, H.** A generalized vortex theory of the screw propeller, NACA-TN-750, 1940.
16 **D'Angelo, S., Berardi, F.,** and **Minisci, E.** Aerodynamic performances of propellers with parametric considerations on the optimal design. *Aeronaut. J.*, 2002, **106**(1060), 313–320.
17 **Wald, Q. R.** The aerodynamic of propellers. *Prog. Aerosp. Sci.*, 2006, **42**(2), 85–128.
18 **Romeo, G., Frulla, G., Cestino, E.,** and **Corsino, G.** HELIPLAT: design, aerodynamic, structural analysis of long-endurance solar-powered stratospheric platform. *J. Aircr.*, 2004, **41**(6), 1505–1520.
19 **Analytical Methods Inc**. *ROTOR user's manual revision*, 1994 (Analytical Methods Inc, Redmond, Washington).

APPENDIX

Notations

D	propeller diameter (m)
FC	fuel cell
h	delay parameter
Ma	Mach number
n	number of blades
opt	optimal propeller
P	shaft power (W)
r/min	revolution per minute
R	propeller radius (m)
Re	Reynolds number
S	propeller disc area (m^2)
S_{body}	cross-sectional area of the body behind the propeller (m^2)
$S_{wet,slip}$	wetted area of the immersed components (m^2)
T	thrust (N)
TAS	true air speed (m/s)
T_{eff}	effective thrust (N)
$T_{isolated}$	thrust without installation effects (N)
v_i	induced velocity at the propeller (m/s)
V_∞	flight speed (m/s)
γ	advance ratio
γ_{eff}	effective advance ratio
η	efficiency
η_i	ideal efficiency
ρ	air density (kg/m^3)
ρ/ρ_0	atmospheric density ratio
τ	thrust coefficient
χ	power coefficient